SEARCH FOR COSMIC DARK MATTER AT CDMS

Laura Baudis*
Stanford University, Stanford, CA 94305

Representing the CDMS Collaboration

ABSTRACT

The dark matter in the Universe might be composed of Weakly Interacting Massive Particles (WIMPs), which are thermal relics of the Big Bang moving non-relativistically at the time of structure formation. Supersymmetric extensions to the Standard Model of particle physics provide an excellent candidate, in form of the neutralino or the lightest supersymmetric particle. Neutralinos can interact via elastic scattering with nuclei in a low background terrestrial detector. The Cryogenic Dark Matter Search (CDMS) experiment uses Ge and Si detectors operated at 20 mK to measure the energy deposited by a recoiling nucleus. Simultaneous measurement of the phonon and the ionization signals allows to discriminate between electron and nuclear recoil events to better than 99.99% down to recoil energies of 10 keV. First results from operating a stack of six ZIP (Z-dependent Ionization and Phonon) detectors at the Stanford Underground Facility shallow location are presented. This tower of ZIP detectors will be the first to be deployed at the deep site location, the Soudan mine in Minnesota, in early 2003.

*lbaudis@stanford.edu

1 Introduction

Astrophysical measurements have progressed to the point that they now provide a reliable inventory of the contents of the universe. Measurements of the first acoustic peak in the angular power spectrum of the Cosmic Microwave Background (CMB)[1] indicate that the total energy density of the universe is near the critical density, $\Omega_{\rm tot} \equiv \rho/\rho_{\rm crit} = 1.0 \pm 0.04$, consistent with the prediction of inflation. Furthermore, separate measurements yield consistent results for the total densities of baryonic and non-baryonic matter, as well as for the amount of the so-called dark energy. The resulting "concordance model" calls for a dark energy density $\Omega_\Lambda = 0.67 \pm 0.06$, a total matter density $\Omega_{\rm M} = 0.33 \pm 0.035$, and a baryon density $\Omega_{\rm b} = 0.04 \pm 0.008$.[2] The fact that stars and other measured, luminous matter account for only $\sim$1% of the total density means that most of the matter, even most of the baryonic matter, consists of unknown, dark components.

The best determination of the cosmological density of baryonic matter is from measurements of near-primordial deuterium in gas clouds towards distant quasars.[3] The theory of Big Bang nucleosynthesis accurately predicts the observed abundance of deuterium only if the baryon density $\Omega_{\rm b}h^2 = 0.020 \pm 0.001$ (where h is related to the Hubble constant by $H_0 \equiv 100h$ km^{-1} s^{-1} Mpc^{-1}). This value of the baryon density also leads to accurate predictions of the primordial abundances of the other lightest elements. The ratio of the amplitudes of odd to even acoustic peaks in the CMB anisotropy spectrum yields a result for the baryon density that is in stunning agreement: $\Omega_{\rm b}h^2 = 0.022^{+0.004}_{-0.003}$. This value is also indicated by (less constraining) measurements of the shape of the power spectrum of matter inhomogeneities[4] combined with measurements of the Hubble constant.[5]

Several measurements give consistent results for the total cosmological matter density. CMB measurements, most notably the height of the first acoustic peak, constrain $\Omega_{\rm M}h^2 = 0.16 \pm 0.04$. Measurements of the shape of the power spectrum of matter inhomogeneities, as determined by large redshift surveys, constrain $\Omega_{\rm M}h = 0.20 \pm 0.03$. These results are in good agreement with those obtained by combining the measured baryon density with measurements of the baryon-to-total mass density ratio in clusters, as determined by X-ray measurements or by measurements of the Sunyaev-Zel'dovich distortion of the CMB. They are further strengthened by observations of distant supernovae,[6] which indicate that $\Omega_\Lambda - \Omega_{\rm M} \approx 0.4$.

The fact that the measured matter density is significantly larger than the measured

baryonic matter density indicates that most of the matter in the universe is non-baryonic particles outside the standard model of particle physics. An excellent candidate for non-baryonic particle dark matter is provided by supersymmetry, which is a well motivated extension to the standard model of particle physics. Although the energy scale where supersymmetry should appear is not *a priori* fixed, in order to solve the problem of mass hierarchies, *i.e.*the stability of the electroweak scale with respect to radiative corrections, the masses of the superpartners must be $\sim$1 TeV.

Several experimental hints favor such weak-scale supersymmetry. The gauge coupling strengths measured by accelerator experiments unify at the GUT scale if the masses of the supersymmetric particles are around 1 TeV.[7] Precision electroweak data favor a light Higgs boson,[8] as predicted in the MSSM, the minimal supersymmetric extension to the standard model. Another hint for new physics at the TeV scale is provided by the new measurement of the anomalous magnetic momentum of the muon.[9,10] The measured 2.6σ deviation from the prediction of the standard model can be well explained by weak-scale supersymmetry,[11,12] which provides contributions to $a_\mu \equiv (g_\mu\text{-}2)/2$ via loops with supersymmetric particles.

In order to prevent baryon- and lepton-number violation in supersymmetric models, the conservation of the so-called R parity is imposed. The R parity takes the value +1 for all standard model particles and -1 for all supersymmetric partners. It implies that sparticles are always produced in pairs, that heavier sparticles decay into lighter ones, and that the lightest supersymmetric particle is stable. The stability of the lightest supersymmetric particle (LSP) renders it an excellent dark matter candidate. The LSP is certainly a neutral, weakly interacting particle, since strong or electromagnetically interacting particles would become bound in anomalous heavy isotopes, which are essentially ruled out by experiments.

A natural possibility for the LSP is the neutralino, a linear combination of the wino, bino, and the two higgsinos, which are the superpartners of the neutral gauge and Higgs bosons. If the neutralino is the LSP and hence is stable, it would be present today as a cosmological relic from the early universe. It would be an example of the general class of Weakly Interacting Massive Particles, or WIMPs,[13] which were once in thermal equilibrium with the early universe, but were "cold," *i.e.*moving non-relativistically at the time of structure formation. The relic density of any WIMP depends on its annihilation cross section, with weak-scale interactions if the dark matter is mainly composed of WIMPs. More detailed calculations indicate that this general statement is accurate for the neutralino in particular: in a large class of supersymmetric models the

abundance of the neutralino is high enough to account for a significant portion of the dark matter in the universe (*i.e.*, to yield a cosmological density between 0.1 and 0.3 of critical density).

For direct dark matter detection experiments, which search for the nuclear recoils produced in elastic scattering of neutralinos from nuclei, it is crucial to estimate the neutralino-nucleon cross section. This cross section, along with the density and velocity distribution of neutralinos in the vicinity of the solar system, determines the expected detection rates in a given detector.

There are many approaches in the literature to evaluate the neutralino-nucleon cross sections. In general, the considered supersymmetric models are classified according to the assumed mechanism for communication of supersymmetry breaking from the hidden to the visible sector. The most basic, yet well motivated approach is the minimal supergravity (mSUGRA) framework, which arises as a low-energy limit of a supergravity theory. In mSUGRA, supersymmetry is broken in the hidden sector of the model and transmitted to the observable sector via gravitational interactions, leading to soft SUSY-breaking masses at the TeV scale. At the GUT scale it leads to a universal scalar mass m_0, a universal gaugino mass $m_{1/2}$, and a common tri-linear coupling A_0. Models under mSUGRA are further characterized by the ratio of the vacuum expectation value of the Higgs duplets, $\tan\beta$, and by the sign of μ, the Higgs mixing parameter in the superpotential, meaning that all sparticle masses and couplings are derived in terms of the four parameters and one sign.

In general, it is found that in mSUGRA the spin-independent neutralino-nucleon cross sections lie between 10^{-6} pb and 10^{-11} pb, with the highest cross sections obtained for the smallest universal gaugino mass $m_{1/2}$ and for the largest $\tan\beta$.

More generic frameworks than mSUGRA are obtained by relaxing some of the unification and other theoretical assumptions. The most phenomenological minimal supersymmetry models define all the parameters directly at the weak scale and make no assumptions at the GUT scale. These models have a higher number of free parameters and in consequence are somewhat less predictive and testable. The general framework results in a wider range of possible neutralino-nucleon cross sections, often bordering or exceeding current limits.

Figure 1 shows the allowed region of parameter space including accelerator constraints on supersymmetry. As shown in the figure, current experiments are at best barely sensitive to some models. The experiments currently being built should be sensitive to a large part of supersymmetry parameter space. Significantly, if the measured

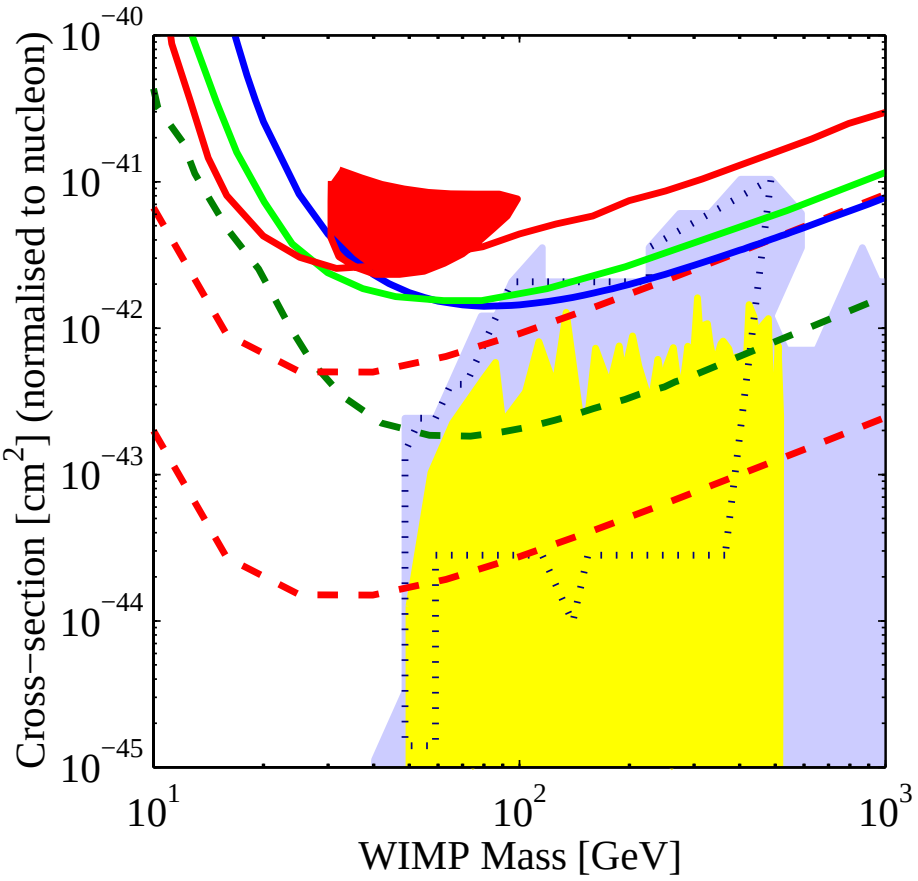

Figure 1: Comparison of theoretical expectations and experimental sensitivities for direct detection of neutralino dark matter. Plotted are the neutralino–nucleon spin-independent cross section vs the neutralino mass. Solid lines (from top to bottom: EDELWEISS,[14] ZEPLIN,[15] CDMS I[16]) are current experimental limits. Dashed curves are projected sensitivities of experiments currently being built (from top to bottom: CRESST, CDMS II at SUF, CDMS II at Soudan) Solid region at upper left is the DAMA annual modulation region.[17] The remaining regions are theoretical expectations. The dark filled region is the region allowed by the MSSM without the muon $g-2$ constraint.[12] Adding the muon $g-2$ constraint reduces the allowed region to the one inside the dotted curve. The lower, lighter region is consistent with the CMSSM.[18] Figure generated with the Dark Matter Plotter.[19]

2.6σ deviation from the prediction of the standard model for the muon anomalous magnetic moment is due to supersymmetry, the neutralino mass must be $< 500\,\mathrm{GeV}$, and neutralino-nucleon cross section must be $> 2 \times 10^{-9}$ pb.[12] In this case, future dark matter projects could be sensitive to the entire allowed parameter region.

2 The CDMS experiment

The Cryogenic Dark Matter Search (CDMS) experiment employs Ge and Si detectors operated at 20 mK to measure the nuclear recoils generated by the hypothetical WIMPs. Simultaneous measurement of the ionization and the phonon energy deposited in a Ge or Si crystal allows to distinguish between a nuclear-recoil event due to a WIMP (or a neutron) and an electron-recoil event, due to the dominant background from radioactive decays. This event by event discrimination is possible due to the fact that for nuclear recoils only about 10% of the recoil energy goes into ionization, while for electron recoils it is about 30%.

The first stage of the experiment, CDMS I, operated at the Stanford Underground Facility (SUF), which is located in a tunnel 10.6 m beneath the Stanford campus. In early 2000, it delivered the most competitive results on WIMP scalar interactions.[16] The second stage, CDMS II, was funded to operate more sophisticated detectors based on Transition Edge Sensors (TESs), the final location being the Soudan Mine in Minnesota, at a depth of about 2080 mwe. The aim is to increase the current CDMS sensitivity by about 2 orders of magnitude.

2.1 The CDMS detectors

A stack of 6 Z-sensitive Ionization- and Phonon-mediated (ZIP) detectors has been operated over the past year at the SUF site. ZIP detectors are made from Ge and Si crystals, 1 cm thick, 7.6 cm in diameter and weighting 250 g and 100 g respectively. Figure 2 shows a picture and a schematic figure of the detectors.

ZIP detectors measure the athermal phonos created in a particle interaction using quasiparticle-trap-assisted electrothermal-feedback transition-edge-sensors.[20] These sensors consist of photolitographically patterned, overlapping thin films of superconductimg aluminum and tungsten, divided into 4 independent channels. Each channel contains a parallel array of 1036 TESs, each coupled to 10 aluminum phonon collection pads. Energy deposited in the crystal leads via anharmonic decay to generation of high-

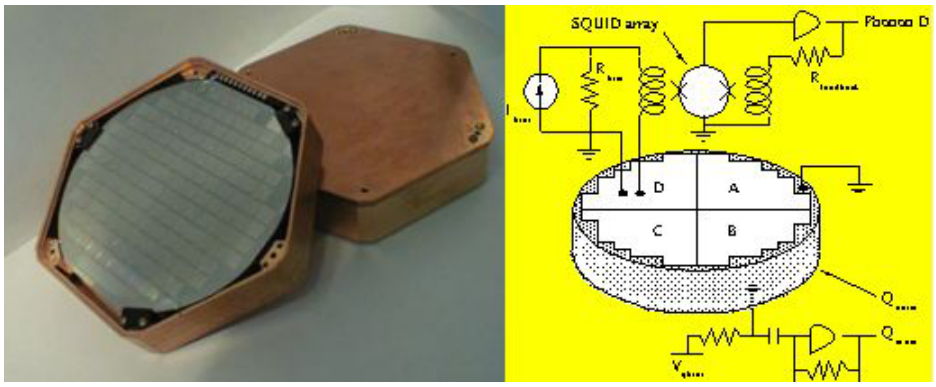

Figure 2: Left: image of a ZIP detector in its copper housing. Right: schematic figure of a detector, showing the 4 phonon and 2 ionization channels with their readout electronics.

frequency, THz phonons, which propagate to the surface where they are absorbed in the superconduction aluminum pads covering 20% of the detector's surface. Here they break Cooper pairs generating quasiparticles which diffuse in about 10μs to the tungsten TES where they become trapped. The quasiparticles lose their potential energy by heating the conduction electrons in the tungsten through electron-electron interactions. The phonons released in the tungsten raise the temperature of the film, increasing its resistance and reducing the current. The TES are voltage biased and the current through them is monitored by a high-bandwidth SQUID array. The sensor temperature is maintained within its superconducting to normal transition via the Joule heating associated with the voltage bias. The intrinsic stability of the voltage bias is due to negative electrothermal feedback. An increase in sensor temperature and thus an increase in sensor resistance causes a decrease in Joule heating, and vice versa.

The TESs are intrinsically very fast, with about 100 ns risetime and 20-40 μs falltimes. The actual ZIP pulses have rise times of 5-15 μs and fall times of about 100 μs, these being dependent on the phonon propagation in the crystal and the quasiparticle diffusion in the aluminum fins. The pulse rise times are sensitive to the phonon arrival times at each of the four quadrants and allow to localize an event in the x-y plane. In addition, events occurring near the detector's surface display faster rise times than bulk events, allowing a fiducial volume cut.

To perform the ionization measurement, a drift field of a few V/cm is applied across the crystal using electrodes deposited on the two faces of each detector. The electrodes are segmented radially, yielding an outer annular guard ring and a central disk-shaped

volume. This design allows to veto events due to radioactive decays in the detector holders. A low-noise amplifier is connected to the biased electrode via a blocking capacitor. The ionization amplifier operates as a current integrator and the observed signal is the voltage drop across a feedback capacitor, which collects a charge proportional to the product of the number of electron hole pairs and the distance they travel across the crystal.

2.2 Cryogenics, low background facility and shields

The CDMS detectors are located inside a large cold volume made of copper, named the Icebox. It consists of six concentric cans, each corresponding to a thermal stage in a modified Oxford S-400 dilution refrigerator. The cryostat is connected to the dilution refrigerator via a copper coldfinger and a set of coaxial copper tubes. Each tube connects one can to the corresponding thermal stage in the refrigerator. The nominal temperatures of the cryostat can are 10 mK, 50 mK, 600 mK, 4 K, 77 K and 300 K. The innermost can has a volume of 30×10^4 cm^3 and can accommodate up to 42 detectors.

Since the predicted rates of WIMP interactions are very low, the CDMS detectors have to be operated in an underground site, in order to minimize the cosmic ray particle flux. However, due to the continuing development of the Ge and Si detectors and the complicated cryogenic technology, the initial experiment was conducted at a local site, in a tunnel 10.6 m below ground level on Stanford campus. A schematic of the Stanford Underground Facility is shown in Figure 3.

The overburden absorbs the hadronic component of cosmic ray showers, and reduces the muon flux by a factor of 5. The large muon flux ($\sim 40\,\mathrm{m}^{-1}\,\mathrm{s}^{-1}$) necessitates an active muon shield to veto the muon-induced gamma and neutron background. This muon-veto made of 4.1 cm thick plastic scintillator paddles surrounds the entire inner, passive shield. Its efficiency has been measured to be higher than 99.99%. The 15 cm thick Pb shield inside the muon-veto attenuates the external photon flux by a factor of 1000. Inside the Pb is a 25 cm thick polyethylene moderator, which surrounds the Icebox and attenuates the neutron flux from the tunnel walls and from muon interactions in the Pb shield. Inside the innermost cryostat can, 1 cm of ancient Pb (low in ^{210}Pb) and about 8 kg of polyethylene further reduce the photon and neutron backgrounds. A drawing of the CDMS shield at SUF is shown in Figure4.

The measured event rate due to photons in the 10-100 keV energy region is about $60\,\mathrm{kg}^{-1}\,\mathrm{d}^{-1}\,\mathrm{keV}^{-1}$ overall and $2\,\mathrm{kg}^{-1}\,\mathrm{d}^{-1}\,\mathrm{keV}^{-1}$ anticoincident with the muon-veto.

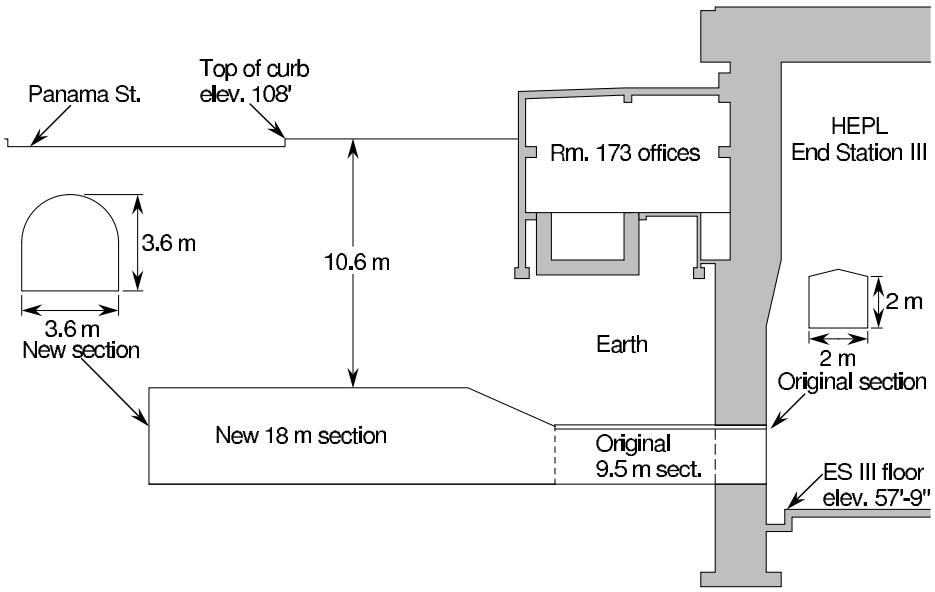

Figure 3: Schematic figure of the Stanford Underground Facility.

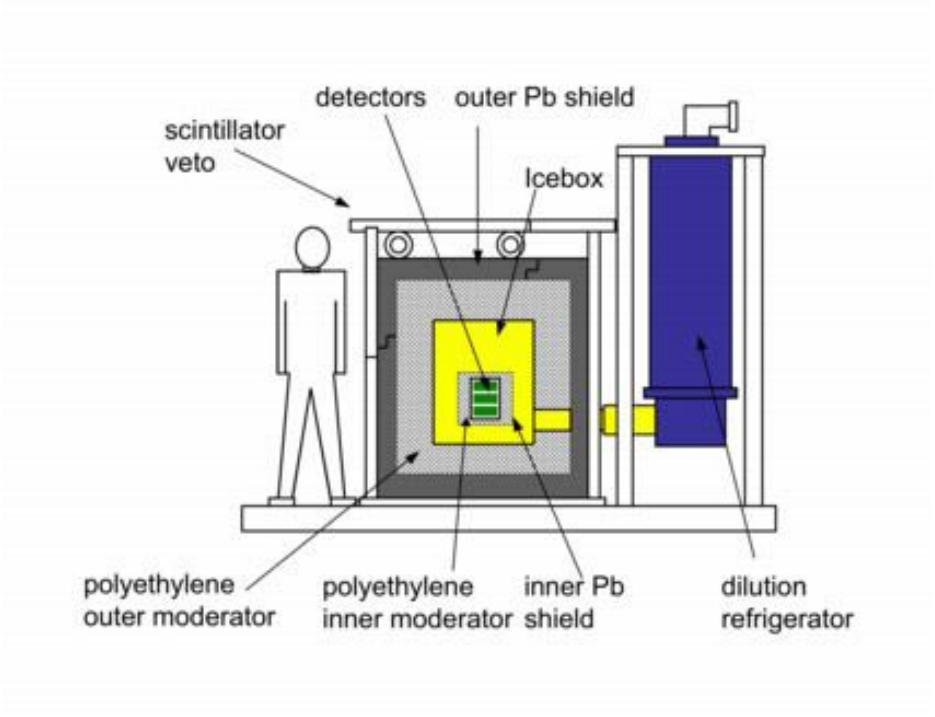

Figure 4: Schematic figure of the CDMS shield at SUF.

This muon anticoincident gamma background is most likely caused by residual radioactivities in the shielding and detector package. It can be reduced to a negligible level due to the excellent ZIP discrimination efficiency against electron recoils, as discussed later.

The main background at the SUF site is generated by high-energy, 'punch-through' neutrons which are produced outside the muon-shield and are moderated to MeV energies yielding keV nuclear recoils in the detectors. This un-reducible neutron background requires operation of the CDMS experiment at a deeper site, eg the Soudan mine in Northern Minnesota. With about 2080 mwe of overburden, the muon flux at the Soudan mine will be reduced by about a factor of 10^4 and the high-energy neutron flux by more than a factor of 100.

2.3 Results from the current run

For the past year, a stack of 6 ZIP (4 Ge and 2 Si) detectors has been operated in the SUF Icebox. The goal of this run was to improve the experiment's sensitivity to WIMPs which had been achieved in 1999 and 2000[16] and to confirm the hypothesis that the dominant background is caused by neutron interactions. Another goal was to test the performance of this first tower of detectors to be deployed at the deep site and to precisely measure and characterize its backgrounds.

Two data sets, taken at 3 V and 6 V ionization voltage bias, each with a total exposure of about 65 livedays have been collected. In the following, preliminary results from the 3 V data set will be presented.

A first rough calibration of the energy scale is done with a ^{137}Cs source, which produces 662 keV gammas able to penetrate the copper cans of the icebox. Comparison of the measured spectra with a detailed Monte Carlo simulation allows to determine the ionization energy scale in both Ge and Si detectors (the 662 keV peak is observed only in the Ge detectors, in the Si detectors the Compton edge of this peak is observed). In the Ge detectors, 2 additional, 'intrinsic' lines in the energy region below 100 keV help to establish the ionization and phonon energy scales. These lines, at 10.37 keV and 66.7 keV, are caused by cosmogenic and neutron activation of some of the Ge isotopes. The energy resolution of the 10.37 keV line is 0.8 keV (FWHM) in the ionization channel and 1 keV (FWHM) in the phonon channel.

After the ionization and phonon energy scales are established, the ability of the detectors to separate nuclear and electron recoils has to be determined. Figure 5 shows the ionization energy against the phonon signal for one Ge and one Si detector. Two

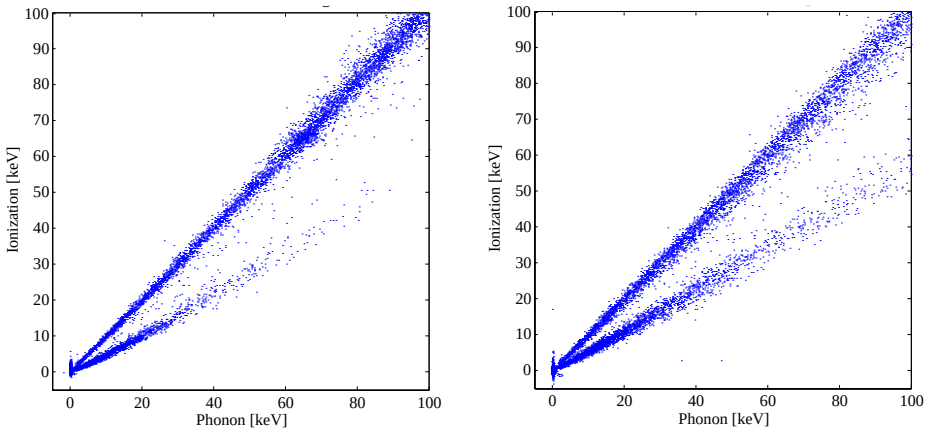

Figure 5: Ionization versus phonon signal for one Ge (left) and one Si (right) detector. Two populations, one caused by electron recoils (steep slope) and one caused by nuclear recoils (shallow slope) are distinguished.

populations, one caused by electron recoils (steep slope) and one caused by nuclear recoils (shallow slope) can be easily distinguished.

Another way of presenting the same data is by defining a quantity named yield, the ratio of ionization to recoil energy. Figure 6 shows the yield parameter as a function of recoil energy. Two populations, or bands, with roughly constant yield are distinguished. The first band, with a yield around 1, is the electron recoil band. Its position and width are determined in a high statistics ^{60}Co calibration. The second band, around a yield value of 1/3, is the nuclear recoil band, as determined in a ^{252}Cf neutron source calibration. Visually, the two bands are well separated down to recoil energies of 5 keV.

To quantify the discrimination factor, the yield parameter is histogrammed for 10 energy bins between 5 keV and 100 keV and the amount of leakage of electron recoil events into the 2σ bound of the neutron recoil band is determined. Figure 7 illustrates the procedure for one of the Ge detectors. The gamma rejection factor is higher than 99.99% between 5 - 100 keV and 99.8% for the lowest energy bin from 5 - 10 keV. These numbers already exceed our requirements for the deep site.

A background more challenging than bulk electron recoils are events occurring near the surface of a detector, in general caused by low energy electrons. These events suffer from a suppressed ionization signal due to a thin 'dead-layer' of the detectors, in which the ionization collection efficiency is reduced. Such events will in general appear in between the two bands in yield versus recoil energy, and their probability to be misidentified as nuclear recoil events is much larger than for bulk electron recoils.

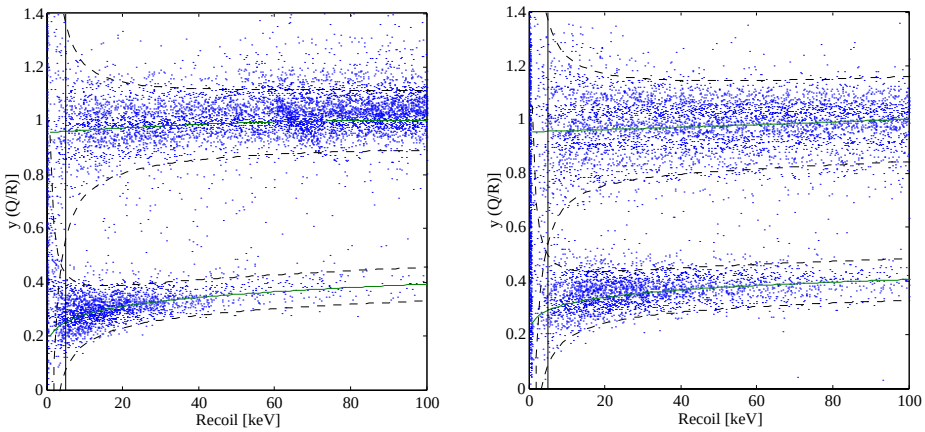

Figure 6: Yield parameter versus recoil energy for one Ge (left) and one Si (right) detector. The band with a yield around 1 is caused by electron recoils, while the band with a yield about 1/3 is caused by nuclear recoils.

Since surface electron recoils show faster phonon pulse risetimes than events occurring in the bulk of a crystal, a combination of cuts in risetime and yield can eliminate a large part of this potential low energy electron background. For the current CDMS run, efforts are underway to determine the amount of surface electron contamination and leakage into the nuclear recoil bands for the ZIP detectors.

Figure 8 shows the muon coincident background of a Si and a Ge ZIP detector. The dominant feature is the electron recoil band, which is populated by muon coincident gammas. This muon coincident gamma background is consistent with the one of previous runs. The nuclear recoil band is dominated by muon coincident neutrons. The nuclear recoil rates are suppressed by a factor of 3 with respect to previous runs, due to the internal polyethylene moderator which was added at the beginning of this run. This is consistent with the suppression factor predicted by Monte Carlo simulations. The muon coincident neutrons are important in providing an 'in situ' calibration of the nuclear recoil band and in testing the stability of this band as a function of time.

The muon anticoincident data set is shown in Figure 9, as ionization yield vs. recoil energy for one Ge and one Si detector. These are events triggering a single detector only, since the WIMP multiple scattering rate is extremely small. The majority of events are in the electron recoil band, although there are some events in the nuclear recoil band and some in between these two bands. Together, the 4 Ge and 2 Si detectors have detected 18 single-scatter nuclear recoils in Ge, 2 single-scatters in Si, and 9 multiply scattered events between the detectors for the 3 V data set. The presence of events in

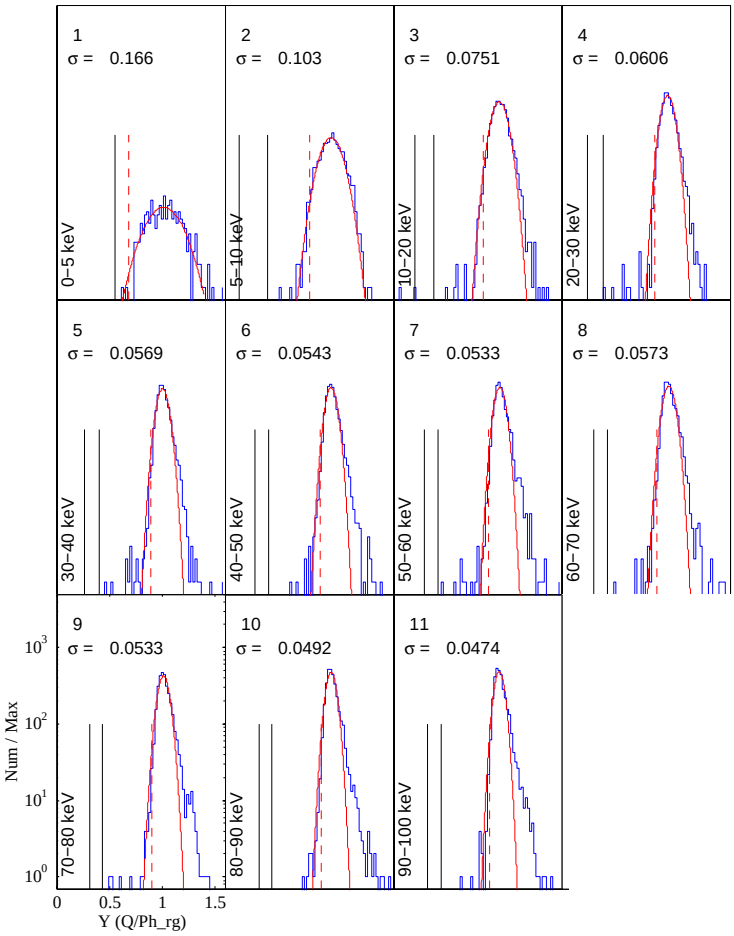

Figure 7: Electron recoil yield histograms for a Ge detector for 10 different energy bins. The electron recoils were generated with an external ^{60}Co source.

the Si detectors and of multiple scattered events, indicates that the events in the nuclear-recoil band are most likely due to neutrons than WIMPs. Monte Carlo simulations of the expected muon anticoincident neutron background at SUF predict 3 single-scatter events in the Si and 8 multiply-scattered events for the same number of Ge single-scatter events observed. Thus the results at SUF are consistent with the entire WIMP signal being due to the un-reducible neutron background present at this shallow site. They are furthermore consistent with neutron Monte Carlo simulations, which predicted about a 2-3 times lower nuclear recoil event rate for the data anticoincident with the muon veto, due to the new internal polyethylene shield.

Work is currently in progress to determine the upper limits on scalar WIMP-nucleon cross sections from this run's data. In order to subtract the residual neutron background,

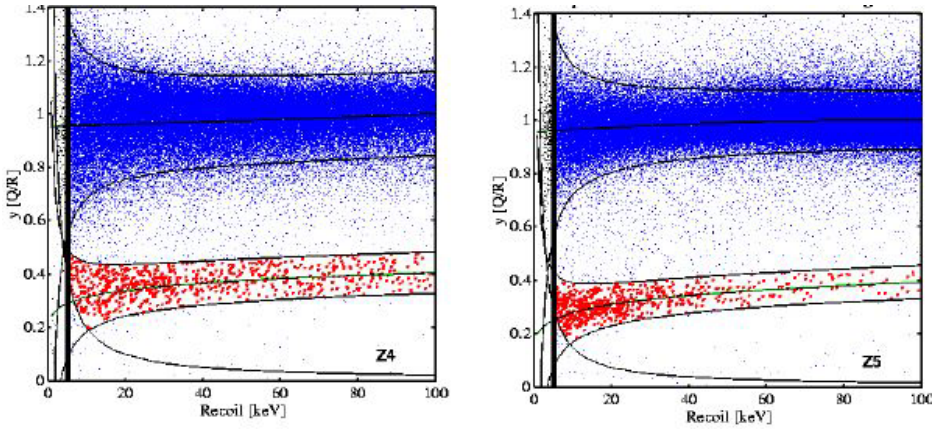

Figure 8: The muon-coincident background, as yield versus recoil energy, for one Si (left) and one Ge (right) ZIP.

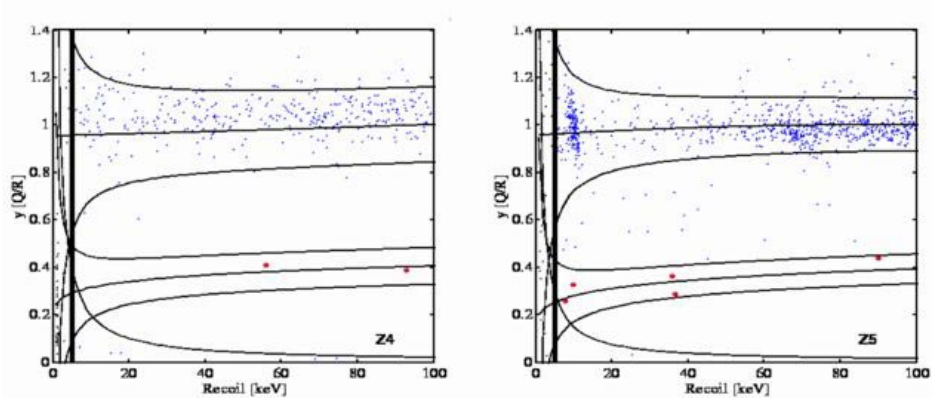

Figure 9: The muon-anticoincident, single-scatter background, as yield versus recoil energy, for one Si (left) and one Ge (right) ZIP.

a careful estimation of possible contaminations of the nuclear recoil band, especially of the multiply-scattered events and of the Si ZIPs data is required. The expected sensitivity at the SUF shallow site is illustrated in Figure 1.

2.4 Conclusions and prospects for the future

The CDMS experiment delivered the most stringent upper limits on scalar WIMP-nucleon interactions in 2001.[16] The EDELWEISS 2002 limit[14] is now more constraining for WIMP masses above 35 GeV. Both experiments rule out the DAMA most likely point[17] at a confidence level higher than 99.9%, under standard WIMP halo and spin-independent cross section assumptions.

The last CDMS run at the Stanford shallow site operated 6 new ZIP detectors with a total exposure larger than 100 livedays. The performance of these 4 Ge and 2 Si detectors exceeded the expectations, the discrimination efficiency against bulk electron recoils being higher than 99.99% (at 90% CL) in the recoil energy region 5-100 keV. The measured background in the nuclear recoil region is consistent will all events being caused by neutron interactions. Due to this un-reducible background at the shallow site, commissioning of the experiment at the Soudan mine deep site is in progress. It is expected that the first stack of 6 detectors will be installed at Soudan early 2003, together with an additional stack of 6 detectors. This second tower is currently being assembled and tested. The prediction for the sensitivity at Soudan is shown in Figure 1. CDMS will be able to probe WIMP-nucleon cross sections down to $\simeq 10^{s}{-}44\mathrm{cm}^2$ for a WIMP mass of 50-100 GeV/c^2.

References

[1] C. B. Netterfield et al. Astrophys.J. **571**, 604-614 (2002), S. Hanany et al., Astrophys. J. Lett. **5**, 545 (2000), C. Pryke et al. Astrophys.J. **568** 46-51 (2002).

[2] M. S. Turner astro-ph/0106035 (2001).

[3] D. Tytler, J. M. O'Meara, N. Suzuki, and D. Lubin, astro-ph/0001318 (2000).

[4] W. J. Percival et al., astro-ph/0105252 (2001).

[5] W. Freedman et al., Astrophys. J. **553**, 47 (2001).

[6] S. Perlmutter et al., Astrophys. J. **517**, 565 (1999).

[7] J. Ellis, S. Kelley and D.V. Nanopoulos, Phys. Lett. B **260** 441 (1990).

[8] http://lepewwg.web.cern.ch/LEPEWWG/.

[9] H. N. Brown et al., Phys. Rev. Lett **86** 2227 (2001).

[10] G.W. Bennett, et al., Muon g-2 Collaboration, Phys. Rev. Lett. **89** 101804 (2002); Erratum-ibid. **89** 129903 (2002).

[11] J. Ellis, D.V. Nanopoulos, and K. A. Olive, hep-ph/0102332.

[12] E. A. Baltz, P. Gondolo, Phys. Rev. Lett. **86** 5004 (2001), E. A. Baltz, P. Gondolo, astro-ph/0207673 (2002).

[13] B. W. Lee and S. W. Weinberg, Phys. Rev. Lett. **39**, 165 (1977).

[14] A. Benoit, Phys.Lett. B **545**, 43-49 (2002)

[15] N. Smith, talk at IDM2002, http://www.shef.ac.uk/ phys/idm2002/talks/pdfs/smith_n.pdf

[16] R. Abusaidi et al., Phys. Rev. Lett. **84**, 25 (2000), CDMS collaboration, astro-ph/0203500 (2002)

[17] R. Bernabei et al., Phys. Lett. **B 480**, 23 (2000)

[18] J. Ellis, A. Ferstl, and K.A. Olive, Phys.Lett. B **532**, 318-328 (2002).

[19] R. Gaitskell, V. Mandic, http://dmtools.berkeley.edu/limitplots/ (2002)

[20] K.D. Irwin et al., Rev. Sci. Instr. **66**, 5322 (1995).